ADVANCED OPTICAL MATERIALS
www.advopticalmat.de

Solvothermal Synthesis and Ultrafast Photonics of Black Phosphorus Quantum Dots

Yanhua Xu, Zhiteng Wang, Zhinan Guo, Hao Huang, Quanlan Xiao, Han Zhang, and Xue-Feng Yu**

Ultrasmall black phosphorus quantum dots (BPQDs) with an average size of 2.1 ± 0.9 nm are synthesized by using a solvothermal method in a *N*-methyl-2-pyrrolidone solution. Verified by femto-second laser Z-scan measurement, BPQDs exhibit excellent nonlinear optical response with a modulation depth of about 36% and a saturable intensity of about 3.3 GW cm^{-2}. By using BPQDs as optical saturable absorber, the ultrashort pulse with a pulse duration of about 1.08 ps centered at a wavelength of 1567.5 nm is generated in mode-locked fiber laser. These results suggest that BPQDs may be developed as another kind of promising nanomaterial for ultrafast photonics.

1. Introduction

Recently, two-dimensional (2D) materials including graphene,[1] transition metal dichalcogenides (TMDs, such as MoS_2, WS_2, etc.),[2] and topological insulators (Bi_2Se_3, Bi_2Te_3, etc.)[3] with outstanding electronic and optical properties[4–8] have been widely used in energy storage device, transistor, photodetectors, and electroluminescent devices.[9–12] Furthermore, some of these nanomaterials are also used as optical absorber for ultrafast photonics, such as passive Q-switcher, optical limiter, and mode locker, because of their broadband nonlinear optical response if under high power laser illumination.[13–17] However, these nanomaterials are limited in its applications for optoelectronic devices because of their intrinsic energy bandgap. Very recently, black phosphorus (BP) as a rising 2D material has raised much attention owing to its relatively higher carrier mobility, and more active photoelectronic response,[18–22] with some emerging applications such as transistors and photodetectors devices.[23–27] Meanwhile, BP is used in vapor sensor, drug delivery, and cellular tracking systems because of its sensitivity and low toxicity.[28–31] Mechanical and liquid exfoliation methods have been adopted to prepare BP nanosheets with different numbers of layers and sizes.[32–34] Due to thickness-dependent bandgap structure of BP which is tunable ranged from 0.3 eV (bulk) to 1.5 eV (monolayer)[26,35,36] and anomalous anisotropy,[37] BP nanosheets show nonlinear saturable absorption properties,[38] and used as the saturable absorber for fiber lasers.[39,40] However, the lateral size and thickness of these BP nanosheets is hardly to be controlled by the liquid exfoliation methods, which limits the investigations of the nonlinear optical properties of the BP with special size.

Recently, ultrasmall BP nanosheets (also called as BP quantum dots, BPQDs) were prepared from the bulk BP crystal using liquid exfoliation methods established by Zhang's group and our group.[41,42] BPQDs exhibit unique electronic and optical properties in association with the quantum confinement and edge effects.[43] However, there remains uninvestigated on the light–matter interaction between laser and BPQDs, and the ultrafast and nonlinear optical properties of BPQDs have not yet been studied.

In this paper, we describe a solvothermal method in *N*-methyl-2-pyrrolidone (NMP) to synthesize ultrasmall BPQDs

Y. Xu, Prof. H. Zhang
Key Laboratory for Micro-/Nano-Optoelectronic Devices of Ministry of Education
School of Physics and Electronics
Hunan University
Changsha 410082, China
E-mail: hzhang@szu.edu.cn

Y. Xu, Dr. Z. Wang, Dr. Z. Guo, Dr. Q. Xiao, Prof. H. Zhang
Shenzhen Key Laboratory of Two-dimensional Materials and Devices/Shenzhen Engineering Laboratory of Phosphorene and Optoelectronics
SZU-NUS Collaborative Innovation Center for Optoelectronic Science and Technology, and Key Laboratory of Optoelectronic Devices and Systems of Ministry of Education and Guangdong Province
Shenzhen University
Shenzhen 518060, China

Y. Xu, Dr. Z. Guo, H. Huang, Dr. Q. Xiao, Prof. X.-F. Yu
Institute of Biomedicine and Biotechnology
Shenzhen Institutes of Advanced Technology
Chinese Academy of Sciences
Shenzhen 518055, China
E-mail: xf.yu@siat.ac.cn

Y. Xu
Key Laboratory of New Electric Functional Materials of Guangxi Colleges and Universities
Guangxi Teachers Education University
Nanning 530023, China

DOI: 10.1002/adom.201600214

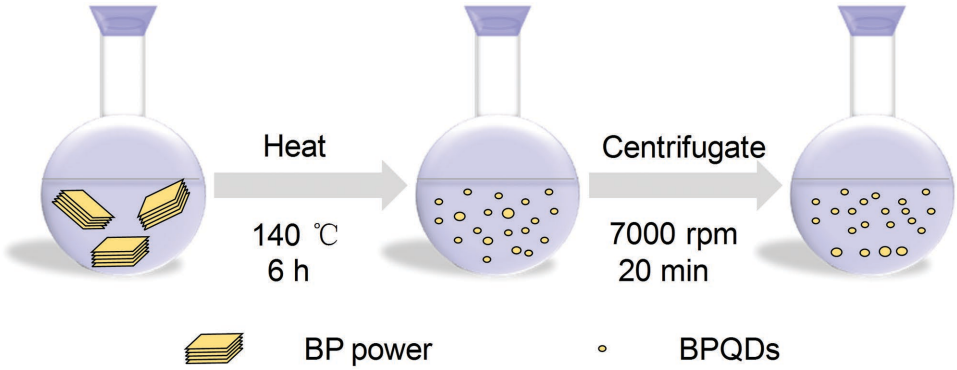

Figure 1. Schematic representation of the synthesis process to prepare BPQDs by using a solvothermal method in NMP.

with an average size of about 2.1 ± 0.9 nm from the bulk form of BP. Verified by laser Z-scan technique, BPQDs are found to exhibit the saturation of optical absorption if under higher laser excitation. Finally, based on the BPQDs saturable absorber, ultrashort laser pulse is generated in mode-locked fiber laser, suggesting that BPQD is another attractive nanomaterial which can be widely applied in optoelectronic devices.

2. Results and Discussions

2.1. Preparation and Characterizations of BPQDs

The ultrasmall BPQDs are prepared in large scale from BP powder by using a solvothermal method. The scheme of the synthesis process is shown in **Figure 1**. In brief, BP crystals were grinded into BP powders, and then added into a flask with saturated NaOH NMP solution while it was under vigorous stirring for 6 h at 140 °C in nitrogen based atmosphere. Given that NMP is a good organic solvent for the exfoliation of 2D materials,[29] the saturated NaOH NMP solution has been verified to be capable of improving the stability of the as-fabricated BP nanosheets.[44] Therefore, the saturated NaOH NMP solution was chosen to produce BPQDs. It is well-known that BP is sensitive to water and oxygen, and easy to be oxidized under visible-light irradiation.[45,46] Consequently, during the whole preparation process, all the experiments were carried out in nitrogen based atmosphere. More details on the synthesis procedure can be found in the Experimental Section. Compared with previously reported mechanical and liquid exfoliation methods, this solvothermal synthesis is facile and controllable to make it possible to produce BPQDs in large scale.

The characterizations of BPQDs are shown in **Figure 2**. Transmission electron microscopy (TEM) was employed to investigate the morphology of BPQDs. The TEM images in Figure 2a,b evidence the existence of ultrasmall BPQDs. Figure 2c shows high-resolution TEM (HRTEM) image of BPQDs in which lattice fringes were 0.573 nm, corresponding to the (020) plane of the BP crystal.[41] According to the statistical TEM analysis of the 100 BPQDs, the average lateral size of BPQDs is about 2.1 ± 0.9 nm as shown in Figure 2d. Three typical Raman peaks of black phosphorus can be seen from Figure 2e, which are corresponding to the out-of-plane vibration mode A_g^1, the in-plane vibration modes B_{2g} and A_g^2, respectively. By using the silicon peak at 520.7 as a calibration standard, it can be seen that three Raman peaks of bulk BP are all red-shifted from BPQDs to different extent, which proves that the average thickness of BPQDs is pretty thin according to our previous report.[45] Figure 2f shows the linear absorption spectrum of BPQDs. 210 mL NMP solution of BPQDs was prepared to investigate the solvothermal method can be used to synthesize BPQDs in large scale, and its photograph is shown as the inset of Figure 2f.

2.2. Nonlinear Optical Absorption Properties of BPQDs

In order to investigate whether BPQDs show better ultrafast optical properties in comparison with BP nanosheets, we performed the Z-scan experiment for BPQDs solution. The NMP solution of BPQDs contained within a cuvette was under the experimental investigation. The experimental setup is shown in **Figure 3**. The incident laser pulses produced by a femto-second laser were controlled by optical attenuators in order to achieve desired average optical power. Then the incident beam was equally divided to two different laser beams. One laser beam as the reference beam was monitored with photodetector 1, while the other laser beam was focused by an objective lens perpendicularly to the solution and further monitored with photodetector 2.

Experimental results of the open aperture Z-scan measurements at 800 nm are shown in **Figure 4**. As shown in Figure 4a, with the increase of the input peak intensity from 35.4 to 354 GW cm^{-2}, the normalized transmittance gradually increases with the approaching of the sample with respect to the focus point ($Z = 0$), which was caused by the optical saturable absorption effect. We further performed a comparison experiment on pure NMP solution, which was verified to be absent of nonlinear saturable absorption effect.[38] These results confirm that the saturable absorption response indeed originates from the intrinsic optical absorption in BPQDs other than NMP solution. BP possesses bandgap from 0.3 to 1.5 eV with thickness of BP from bulk degrading to monolayer.[36] Therefore, under an excitation of 800 nm femto-second laser, one photon (1.55 eV) is enough to excite an electron from the valence band to the conduction band in the BPQDs. In the NMP solution of BPQDs, the absorption coefficients $\alpha(I)$ consist of two parts

$$\alpha(I) = \alpha_0 + \alpha I \quad (1)$$

Adv. Optical Mater. 2016,
DOI: 10.1002/adom.201600214

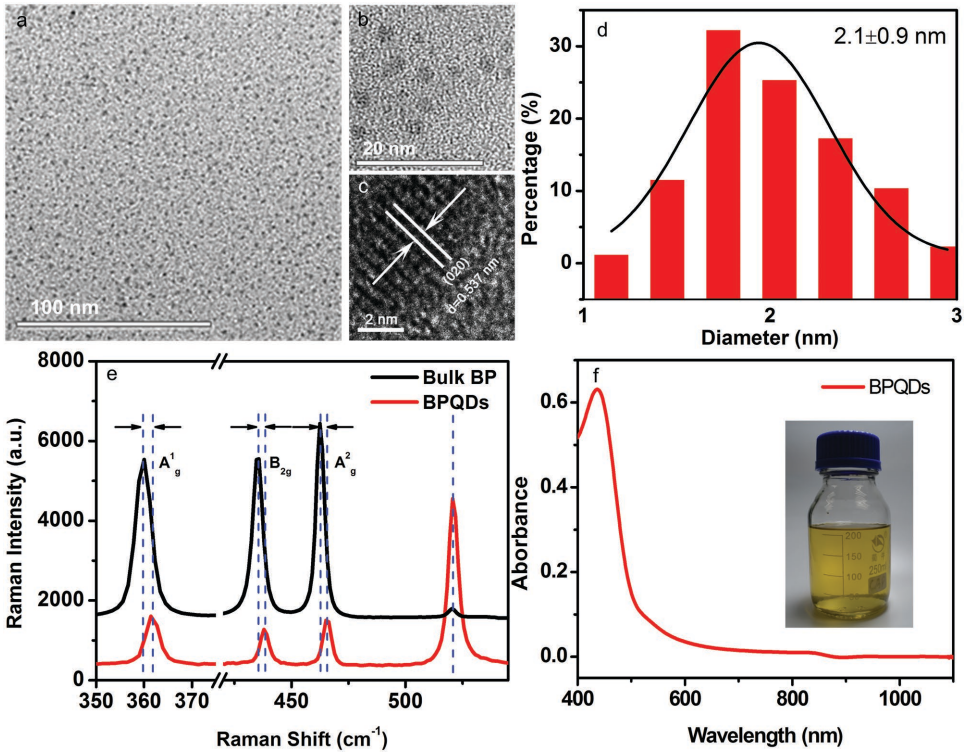

Figure 2. Characterizations of BPQDs. a) TEM image. b) Magnified TEM image. c) HRTEM image. d) Statistical analysis of the lateral sizes of 100 BPQDs determined by TEM. e) Raman spectra. f) Absorption spectrum and inset photograph of the NMP solution of BPQDs.

where I is the input optical intensity, α_0 is the linear absorption coefficient, and α is the nonlinear absorption coefficient. According to the nonlinear theory,[47] we fitted the Z-scan curves in Figure 4a with the following approximate equation

$$T(Z) = \sum_{n=0}^{\infty} (-\alpha I_0 L_{\text{eff}})^n / (1 + Z^2/Z_0^2)^n \quad (n+1)^{3/2} \approx 1 - \alpha I_0 L_{\text{eff}} / 2^{3/2} (1 + Z^2/Z^2 Z_0^2) \quad (2)$$

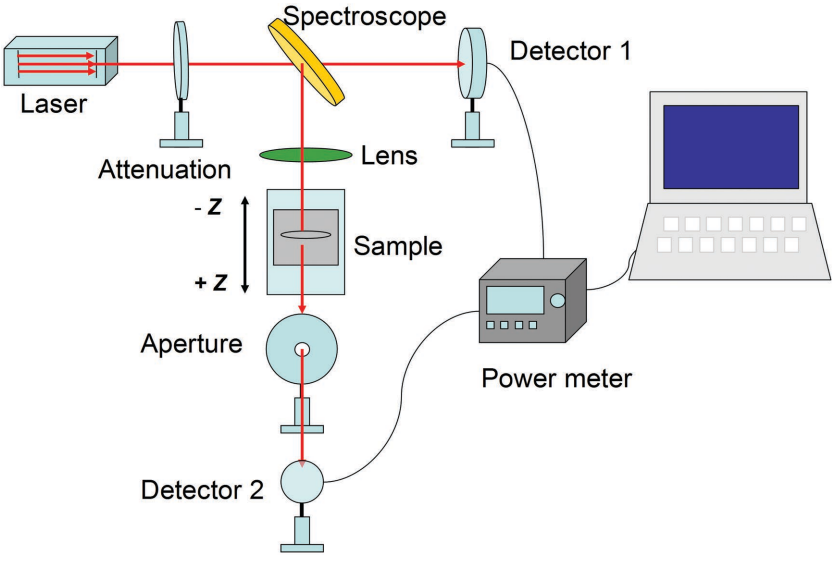

Figure 3. The experimental setup of open aperture Z-scan technique at 800 nm.

where $T(Z)$ is the normalized transmittance, I_0 is peak on-axis intensity at focus, Z is the position of sample with respect to the focal position, Z_0 is the diffraction length of the beam, $L_{\text{eff}} = (1 - e^{-\alpha L})/\alpha_0$ is the effective length, and L is the length of the sample. At 800 nm band, the linear absorption of the BPQDs is about 65%, and the corresponding linear absorption coefficient $\alpha_0 \approx 4.3$ cm^{-1}. We fitted the average value of α which is found to be about $-(5.9 \pm 0.12) \times 10^{-3}$ cm GW^{-1} at different peak intensities.

In Figure 4b, we fitted the data with the input intensity I based on the saturable absoption model for one photon absorption.[48] The transmittance T has a relation with input optical intensity as

$$T = 1 - A_s / (1 + I / I_{\text{sat}}) - A_{\text{ns}} \quad (3)$$

where A_s is the modulation depth, A_{ns} is the non-saturable components, I_{sat} is the saturable intensity, and I in the incident light intensity. The experimental data match with Equation (3). By fitting the experimental data, the modulation depth and the saturable intensity are found to be about 36% and 3.3 GW cm^{-2}, respectively. BPQDs have higher modulation depth and lower saturable intensity in contrast with BP nanosheets.[38]

To evaluate the nonlinear saturable property of BPQDs, we also repeated the Z-scan experiment at 800 nm for BP

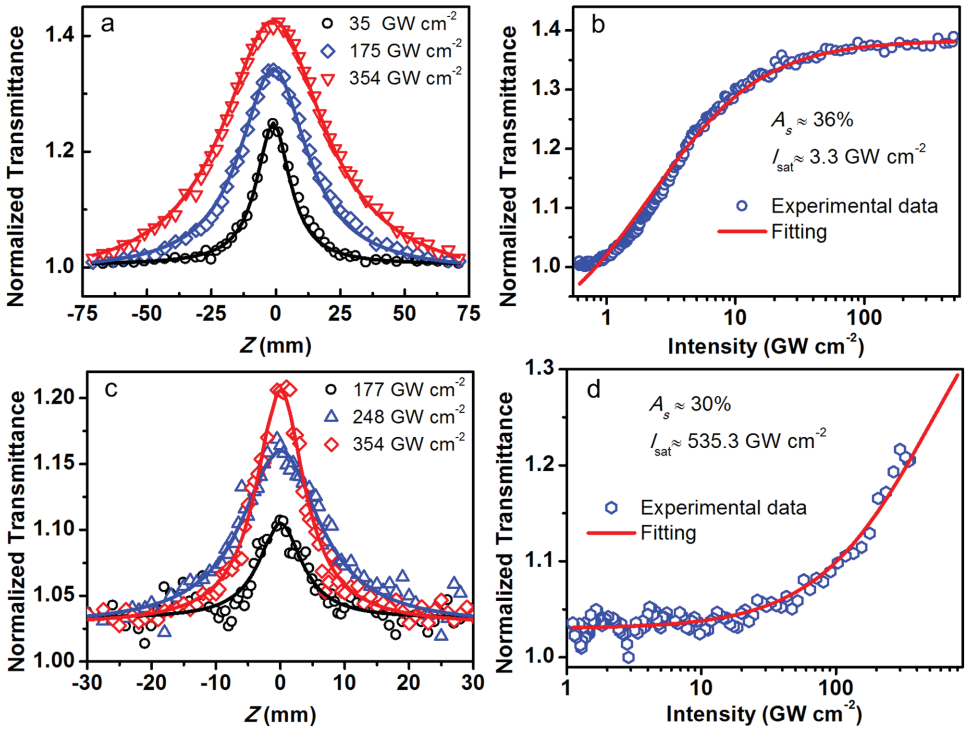

Figure 4. The experimental results and fittings measured by Z-scan technique at 800 nm. The open Z-scan curves for a) BPQDs and c) BP nanosheets. The normalized transmittance and input peak intensity for b) BPQDs and d) BP nanosheets.

nanosheets. The measured results are shown in Figure 4c,d that were fitted by using Equations (2) and (3). The average value of the nonlinear absorption coefficient α is about $-(2.5 \pm 0.19) \times 10^{-3}$ cm GW^{-1} at different peak intensities, and the fitted modulation depth is about 30%, while the saturable intensity is about 535.3 GW cm^{-2}. It should be noted that BPQDs have lower saturable intensity than BP nanosheets while they have similar modulation depths. It mainly benefits from the ultrasmall size structure of BPQDs that changes the energy bandgap of few layer BP nanosheets due to the quantum confinement effect, which correspondingly alters the optical properties of BPQDs. **Table 1** shows the nonlinear saturable properties of different materials, in contrast with BP nanosheets, BPQDs have better saturable absorption properties, and may be considered as another choice of nonlinear optical material for ultrafast photonics.

2.3. Applications toward Ultrafast Photonics

Since that the nonlinear saturable property of BPQDs has been investigated, the use of BPQDs as a saturable absorber for mode-locked fiber laser is attractive. The schematic of the passively mode-locked fiber laser based on BPQDs saturable absorber is shown in **Figure 5**. The cavity length is about 13.39 m. A piece of 3.0 m erbium-doped fiber with group

Table 1. Nonlinear saturable properties of different materials.

Materials	λ [nm]	Duration time	α [cm GW^{-1}]	A_s [%]	I_{sat} [GW cm^{-2}]
PbS QDs	1060	50 ps	45.7[49]	N/A	N/A
PbS QDs	530	50 ps	−50[49]	N/A	N/A
Fe_2O_3 QDs	1060	15 ns	0.82[50]	N/A	N/A
GaAs QDs	1060	100 ps	30[51]	N/A	N/A
BPQDs	800	100 fs	$-(2.5 \pm 0.19) \times 10^{-3}$[a)]	36	3.3
BP	800	100 fs	$-(4.08 \pm 0.11) \times 10^{-3}$[38]	13.3	647.7 ± 60
MoS_2	1030	340 fs	66 ± 4[52]	N/A	65
WS_2	800	40 fs	−397 ± 40[52]	N/A	N/A
Bi_2Se_3	800	100 fs	N/A[53]	88	32
Graphene	1550	1 fs	N/A[13]	66.5–6.2	$(0.71–0.61) \times 10^{-3}$

[a)]The current paper.

Adv. Optical Mater. 2016,
DOI: 10.1002/adom.201600214

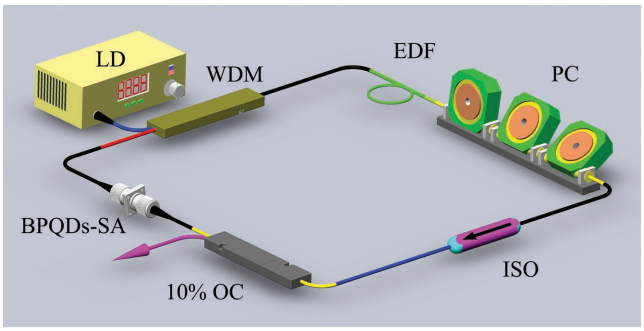

Figure 5. The schematic of the passively mode-locked fiber laser based on BPQDs saturable absorber. LD: laser diode. EDF: erbium-doped fiber. PC: polarization controller. PC: polarization controller. ISO: polarization independent isolator. OC: output coupler. BPQDs-SA: BPQDs based saturable absorber.

velocity dispersion of 10 (ps nm^{-1}) km^{-1} is used as the gain medium that is pumped by a 980 nm laser diode using a 980/1550 nm wavelength division multiplexer. An intra-cavity polarization controller is used to fine-tune the linear birefringence of the laser. A polarization independent isolator is used to force the unidirectional circulation of the laser. The BPQDs based saturable absorber is used as a mode locker. The mode-locked pulse is outputted by a 10% optical coupler and detected by a spectrum analyzer (Ando AQ-6317B), an optical spectrum analyzer (N9322C), and an oscilloscope (DS09404A). The total cavity group velocity dispersion is estimated to be –0.277 ps^2 with 10.39 m optical pigtail (single mode fiber), whose group velocity dispersion is 18 (ps nm^{-1}) km^{-1}.

The fabrication process of the BPQDs based saturable absorber is described as follows. First, the BPQDs dispersion solution in NMP and the powder of polyvinylidene fluoride (PVdF) were mixed with ultrasonicating for 30 min to get the PVdF-BPQDs slurry. Second, the slurry is cast and punched on an aluminum foil to form the PVdF-BPQDs composite film over the aluminum foil with evaporating at 80 °C for 6 h. Finally, the saturable absorber was successfully fabricated by transferring the composite between two fiber connectors.

By placing the as-fabricated BPQDs saturable absorber inside the fiber laser cavity, the self-starting mode-locked operation could be obtained at a pump power of 50 mW, as shown in **Figure 6**. The central spectrum of the mode-locked pulse is located at 1567.5 nm with a 3 dB spectral bandwidth of 2.4 nm. Clear sidebands have been observed in Figure 6a, indicating that the obtained output pulse is a soliton pulse. Figure 6b shows the measured oscilloscope trace of the output pulse-train with a pulse-to-pulse interval of 65.7 ns, which corresponds to a cavity repetition rate of 15.22 MHz. Furthermore, the inset of Figure 6b characterizes its long range stability. Figure 6c

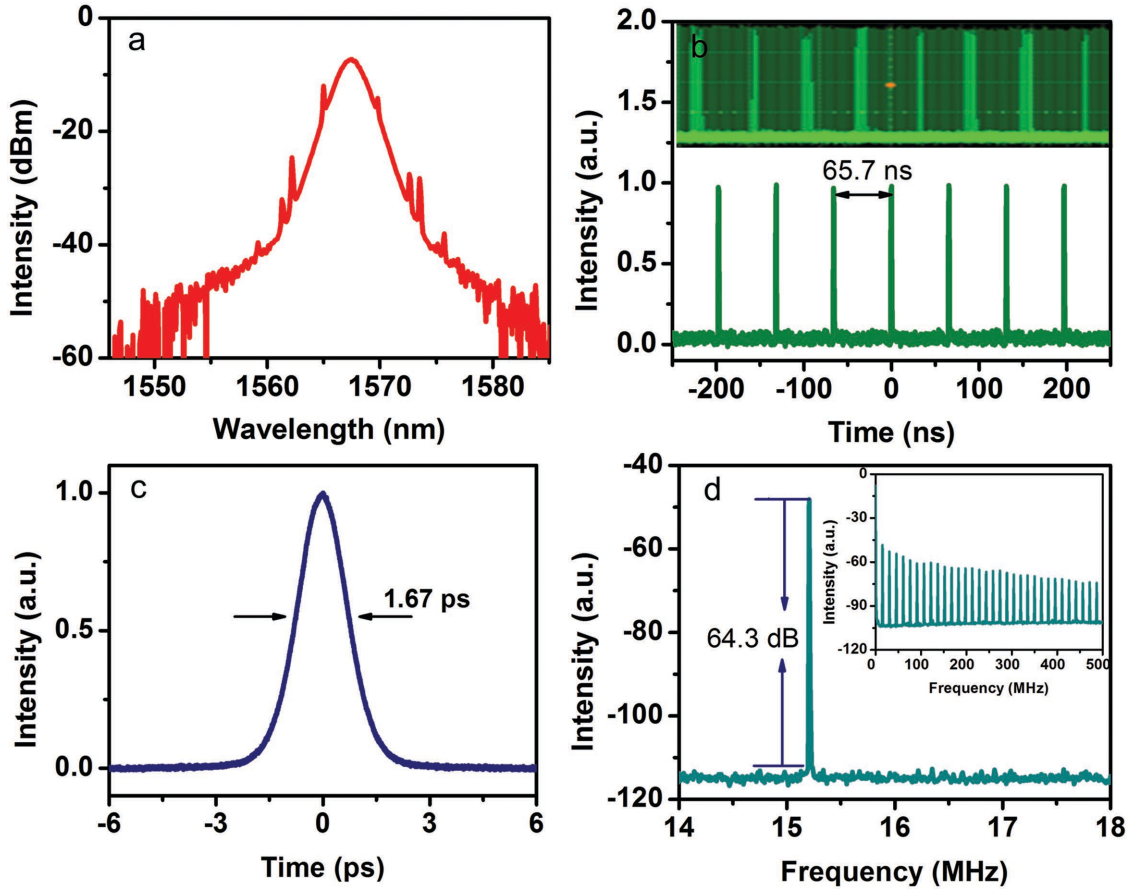

Figure 6. a) Optical spectrum, b) pulse train, c) autocorrelation trace, and d) the radio frequency spectrum (inset: the wideband RF spectrum) of the mode-locked pulses.

illustrates a measured autocorrelation trace of the mode-locked pulses with a pulse duration of 1.67 ps, which suggests a real pulse duration of 1.08 ps if by multiplying a factor of 0.65 (for sech^2-pulse profile). The corresponding time-bandwidth product is calculated to be 0.316. The radio frequency spectrum of the laser with a repetition rate of 15.25 MHz is depicted in Figure 6d, which is well consistent with a cavity length of 13.11 m. The noise ratio of electrical signal at 15.25 MHz is about 64.3 dB if measured with 10 Hz resolution bandwidth.

3. Conclusion

In summary, we have demonstrated a solvothermal method for large-scale synthesis of BPQDs with an average size of 2.1 ± 0.9 nm. By performing femto-second Z-scan measurement, it has been found that BPQDs show excellent nonlinear optical saturable absorption with a modulation depth of 36% and a saturable intensity of about 3.3 GW cm^{-2}. Taking advantages of the nonlinear optical property of BPQDs, a kind of novel optical saturable absorber based on BPQDs has been designed, which can deliver the generation of ultrashort pulse at a wavelength of 1567.5 nm in an Er-doped fiber laser. Our results suggest that BPQDs can be developed as a good candidate for ultrafast photonics devices.

4. Experimental Section

Materials: BP crystals of high-purity were purchased from Smart Elements, NMP (99.5%) and sodium hydroxide (NaOH) were obtained from Aladdin Reagents. All the chemicals were used as received without further purification.

Preparation of BPQDs: BP crystals were first grinded into black phosphorus powder, and added into a bottle with NMP solution. Typically, 20 mg of black phosphorus crystals can get 20 mL BP NMP solution. Then 20 mL of BP NMP solution, 180 mL of NMP, and 200 mg NaOH were added in a flask and kept under vigorous stirring for 6 h at 140 °C. The experimental procedure was performed in a nitrogen environment. Afterward, the resulting suspensions were centrifuged for 20 min at 7000 rpm to separate the centrifugate and supernatant. The light yellow supernatant was the NMP solution of BPQDs.

Characterization: TEM and HRTEM images were taken on the Tecnai G2 F20 S-Twin transmission electron microscope at an acceleration volltage of 200 kV. The absorption spectra were acquired on a TU-1810 UV–visible–NIR spectrophotometer (Purkinje General Instrument Co. Ltd. Beijing, China). Raman scattering was performed on the Horiba Jobin-Yvon LabRam HR-VIS high-resolution confocal Raman microscope equipped with a 633 nm laser as the excitation source at room temperature and a XYZ motorized sample stage controlled by LabSpec software.

Z-Scan Experiment: The incident laser was obtained from a Coherent femto-second laser (center wavelength: 800 nm, pulse duration: 100 fs, 3 dB spectral width: 15 nm, and repetition rate: 1 kHz). The focal length of the lens is 500 mm, and the incident beam waist is fitted to be about 30 μm.

Acknowledgements

Y.X. and Z.W. contributed equally to this work. This work was partially supported by the National Natural Science Fund of China (Grant No. 61435010), National Natural Science Foundation of Guangdong Province of China (Grant No. 2014A030310416), the Science and Technology Innovation Commission of Shenzhen (KQTD2015032416270385), and the Science and Technology Innovation Commission of Shenzhen (JCYJ20150625103619275).

Received: March 27, 2016
Revised: April 18, 2016
Published online:

[1] A. K. Geim, K. S. Novoselov, *Nat. Mater.* **2007**, *6*, 183.
[2] K. F. Mak, C. Lee, J. Hone, J. Shan, T. F. Heinz, *Phys. Rev. Lett.* **2010**, *105*, 136805.
[3] a) J. E. Moore, *Nature* **2010**, *464*, 194; b) M. Z. Hasan, C. L. Kane, *Rev. Mod. Phys.* **2010**, *82*, 3045; c) D. Hsieh, D. Qian, L. Wray, Y. Xia, Y. S. Hor, R. J. Cava, M. Z. Hasan, *Nature* **2008**, *452*, 970.
[4] A. A. Balandin, S. Ghosh, W. Bao, I. Calizo, D. Teweldebrhan, F. Miao, C. N. Lau, *Nano Lett.* **2008**, *8*, 902.
[5] G. X. Ni, H. Z. Yang, W. Ji, S. J. Baeck, C. T. Toh, J. H. Ahn, B. Özyilmaz, G. X. Ni, H. Z. Yang, W. Ji, *Adv. Mater.* **2014**, *26*, 1081.
[6] J. A. Wilson, A. D. Yoffe, *Adv. Phys.* **1969**, *18*, 193.
[7] L. Sun, Z. Lin, J. Peng, J. Weng, Y. Huang, Z. Luo, *Sci. Rep.* **2014**, *4*, 4794.
[8] S. B. Lu, C. J. Zhao, Y. H. Zou, S. Q. Chen, Y. Chen, Y. Li, H. Zhang, S. C. Wen, D. Y. Tang, *Opt. Express* **2013**, *21*, 2072.
[9] M. W. Lin, C. Ling, Y. Y. Zhang, H. J. Yoon, M. M. C. Cheng, L. A. Agapito, N. Kioussis, N. Widjaja, Z. X. Zhou, *Nanotechnology* **2011**, *22*, 265201.
[10] X. Li, X. Wang, L. Zhang, S. Lee, H. Dai, *Science* **2008**, *319*, 1229.
[11] Y. Zhang, J. Ye, Y. Matsuhashi, Y. Iwasa, *Nano Lett.* **2012**, *12*, 1136.
[12] H. Zhu, C. A. Richter, E. Zhao, J. E. Bonevich, W. A. Kimes, H. J. Jang, H. Yuan, H. T. Li, A. Arab, O. Kivillov, J. E. Maslar, D. E. Ioannou, Q. L. Li, *Sci. Rep.* **2013**, *3*, 1757.
[13] Q. L. Bao, H. Zhang, Y. Wang, Z. Ni, Y. Yan, Z. X. Shen, K. P. Loh, D. Y. Tang, *Adv. Funct. Mater.* **2009**, *19*, 3077.
[14] H. Zhang, Q. L. Bao, D. Y. Tang, L. M. Zhao, K. P. Loh, *Appl. Phys. Lett.* **2009**, *95*, 141103.
[15] J. Du, Q. K. Wang, G. B. Jiang, C. W. Xu, C. J. Zhao, Y. J. Xiang, Y. Chen, S. C. Wen, H. Zhang, *Sci. Rep.* **2014**, *4*, 6346.
[16] H. Zhang, S. B. Lu, J. Zheng, J. Du, S. C. Wen, D. Y. Tang, K. P. Loh, *Opt. Express* **2014**, *22*, 7249.
[17] Z. Q. Luo, Y. Z. Huang, J. Weng, H. H. Cheng, Z. Q. Lin, B. Xu, Z. P. Cai, H. Y. Xu, *Opt. Express* **2013**, *21*, 29516.
[18] H. O. H. Churchill, P. Jarillo-Herrero, *Nat. Nanotechnol.* **2014**, *9*, 330.
[19] S. P. Koenig, R. A. Doganov, H. Schmidt, A. H. Castro Neto, B. Özyilmaz, *Appl. Phys. Lett.* **2014**, *104*, 103106.
[20] S. Chintalapati, L. Shen, Q. H. Xiong, Y. P. Feng, *Appl. Phys. Lett.* **2015**, *107*, 072401.
[21] T. Low, A. S. Rodin, A. Carvalho, Y. J. Jiang, H. Wang, F. N. Xia, A. H. Castro Neto, *Phys. Rev. B* **2014**, *90*, 075434.
[22] H. Asahina, A. Morita, *J. Phys. C: Solid State Phys.* **1984**, *17*, 1839.
[23] M. Buscema, D. J. Groenendijk, S. I. Blanter, G. A. Steele, H. S. J. van der Zant, A. Castellanos-Gomez, *Nano Lett.* **2014**, *14*, 3347.
[24] L. K. Li, Y. J. Yu, G. J. Ye, Q. Q. Ge, X. D. Ou, H. Wu, D. L. Feng, X. H. Chen, Y. B. Zhang, *Nat. Nanotechnol.* **2014**, *9*, 372.
[25] M. Engel, M. Steiner, P. Avouris, *Nano Lett.* **2014**, *14*, 6414.
[26] F. N. Xia, H. Wang, Y. C. Jia, *Nat. Commun.* **2014**, *5*, 4458.
[27] X. M. Wang, A. M. Jones, K. L. Seyler, V. Tran, Y. C. Jia, H. Zhao, H. Wang, L. Yang, X. D. Xu, F. N. Xia, *Nat. Nanotechnol.* **2015**, *10*, 517.
[28] N. M. Latiff, W. Z. Teo, Z. Sofer, A. C. Fisher, M. Pumera, *Chem. Eur. J.* **2015**, *21*, 13991.

[29] C. C. Mayorga-Martinez, Z. Sofer, M. Pumera, *Angew. Chem., Int. Ed.* **2015**, *54*, 14317.
[30] Z. Sofer, D. D. Bouša, J. Luxa, V. Mazanek, M. Pumera, *Chem. Commun.* **2016**, *52*, 1563.
[31] H. U. Lee, S. Y. Park, S. C. Lee, S. Choi, S. Seo, H. Kim, J. Won, K. S. Kang, H. G. Park, H.-S. Kim, H. R. An, K.-H. Jeong, Y.-C. Lee, J. Lee, *Small* **2016**, *12*, 214.
[32] A. Castellanos-Gomez, L. Vicarelli, E. Prada, J. O. Island, K. L. Narasimha-Acharya, S. I. Blanter, D. J. Groenendijk, M. Buscema, G. A. Steele, J. V. Alvarez, *2D Mater.* **2014**, *1*, 025001.
[33] J. R. Brent, N. Savjani, E. A. Lewis, S. J. Haigh, D. J. Lewis, P. O'Brien, *Chem. Commun.* **2014**, *50*, 13338.
[34] J. Kang, J. D. Wood, S. A. Wells, J. H. Lee, X. L. Liu, K. S. Chen, M. C. Hersam, *ACS Nano* **2015**, *9*, 3596.
[35] D. Warschauer, *J. Appl. Phys.* **1963**, *34*, 1853.
[36] V. Tran, R. Soklaski, Y. F. Liang, L. Yang, *Phys. Rev. B* **2014**, *89*, 235319.
[37] Z. Sofer, D. Sedmidubsky, Š. Huber, J. Luxa, D. Bouša, C. Boothroyd, M. Pumera, *Angew. Chem., Int. Ed.* **2016**, *55*, 3382.
[38] S. B. Lu, L. L. Miao, Z. N. Guo, X. Qi, C. J. Zhao, H. Zhang, S. C. Wen, D. Y. Tang, D. Y. Fan, *Opt. Express* **2015**, *23*, 11183.
[39] Y. Chen, G. B. Jiang, S. Q. Chen, Z. N. Guo, X.-F. Yu, C. J. Zhao, H. Zhang, Q. L. Bao, S. C. Wen, D. Y. Tang, D. Y. Fan, *Opt. Express* **2015**, *23*, 12823.
[40] H. R. Mu, S. H. Lin, Z. C. Wang, S. Xiao, P. F. Li, Y. Chen, H. Zhang, H. F. Bao, S. P. Lau, C. X. Pan, D. Y. Fan, Q. L. Bao, *Adv. Opt. Mater.* **2015**, *3*, 1447.
[41] X. Zhang, H. M. Xie, Z. D. Liu, C. L. Tan, Z. M. Luo, H. Li, J. D. Lin, L. Q. Sun, W. Chen, Z. C. Xu, L. H. Xie, W. Huang, H. Zhang, *Angew. Chem., Int. Ed.* **2015**, *54*, 3653.
[42] Z. B. Sun, H. H. Xie, S. Y. Tang, X.-F. Yu, Z. N. Guo, J. D. Shao, H. Zhang, H. Huang, H. Y. Wang, P. K. Chu, *Angew. Chem.* **2015**, *127*, 11688.
[43] K. A. Ritter, J. W. Lyding, *Nat. Mater.* **2009**, *8*, 235.
[44] Z. N. Guo, H. Zhang, S. B. Lu, Z. T. Wang, S. Y. Tang, J. D. Shao, Z. B. Sun, H. H. Xie, H. Y. Wang, X.-F. Yu, P. K. Chu, *Adv. Funct. Mater.* **2015**, *25*, 6996.
[45] A. Ziletti, A. Carvalho, D. K. Campbell, D. F. Coker, A. H. Castro Neto, *Phys. Rev. Lett.* **2015**, *114*, 046801.
[46] Y. T. Zhao, H. Y. Wang, H. Huang, Q. L. Xiao, Y. H. Xu, Z. N. Guo, H. H. Xie, J. D. Shao, Z. B. Sun, W. J. Han, X.-F. Yu, P. H. Li, P. K. Chu, *Angew. Chem.* **2016**, *55*, 5003.
[47] M. Sheik-Bahae, A. A. Said, T. H. Wei, D. J. Hagan, E. W. Van Stryland, *IEEE J. Quantum Electron.* **1990**, *26*, 760.
[48] E. Garmire, *IEEE J. Sel. Top. Quantum Electron.* **2000**, *6*, 1094.
[49] B. L. Yu, G. S. Yin, C. S. Zhu, F. X. Gan, *Opt. Mater.* **1998**, *11*, 17.
[50] B. L. Yu, C. S. Zhu, F. X. Gan, X. C. Wu, G. L. Zhang, G. Q. Tang, W. J. Chen, *Opt. Mater.* **1997**, *8*, 249.
[51] B. L. Justus, R. J. Tonucci, A. D. Berry, *Appl. Phys. Lett.* **1992**, *61*, 3151.
[52] S. F. Zhang, N. N. Dong, N. McEvoy, M. O'Brien, S. Winters, N. C. Berner, C. Y. Yim, X. Y. Zhang, Z. H. Chen, L. Zhang, G. S. Duesberg, J. Wang, *ACS Nano* **2015**, *9*, 7142.
[53] Y. H. Xu, H. H. Xie, G. B. Jiang, L. L. Miao, K. Wang, S. Y. Tang, X.- F. Yu, H. Zhang, Q. L. Bao, *Opt. Commun.* **2015**, doi: 10.1016/j.optcom.2015.11.061.